AAPS PharmSciTech, Vol. 12, No. 3, September 2011 (© 2011)
DOI: 10.1208/s12249-011-9654-6

Research Article

Macrophage-Specific Targeting of Isoniazid Through Mannosylated Gelatin Microspheres

Sanjay Tiwari,[1] Adya P. Chaturvedi,[2] Yamini B. Tripathi,[2] and Brahmeshwar Mishra[1,3]

Received 3 February 2011; accepted 20 June 2011; published online 6 July 2011

Abstract. Active targeting of drug molecules can be achieved by effective attachment of suitable ligands to the surface of carriers. The present work was attempted to prepare mannosylated gelatin microspheres (m-GMs) so as to achieve targeted delivery of isoniazid (INH) to alveolar macrophages (AMs) and maintain its therapeutic concentration for prolonged period of time. Microspheres were prepared by emulsification solvent extraction method and evaluated for physicochemical characteristics, drug release, *ex vivo* drug uptake by AMs and pharmacokinetic characteristics. Fourier transform infrared spectroscopy and nuclear magnetic resonance spectral analysis confirmed that mannosylation took place through Schiff base formation between aldehyde and amino groups of mannose and gelatin, respectively. Prepared microspheres offered suitable physicochemical characteristics for their delivery to AMs. Their average size was about 4 μm and drug entrapment efficiency of 56% was achieved with them. *Ex vivo* uptake results indicated that in comparison to plain microspheres, m-GMs were selectively uptaken and were found to be associated with phago-lysosomal vesicles of AMs. Pharmacokinetic studies showed the formulation could maintain the therapeutic concentration of INH for prolonged period of time even with a reduced clinical dose. m-GMs were found to be stable in broncheo-alveolar lavage fluid. The study concluded that ligand decorated carriers could be a potential strategy to improve the therapeutic properties of INH.

KEY WORDS: active targeting; alveolar macrophages; isoniazid; mannosylated gelatin microspheres.

INTRODUCTION

Alveolar macrophages (AMs) are the pivotal regulators of immunological homeostasis and key effector cells in the first-line host defense (1). In response to invasion, they release a variety of secretory products which in turn trigger phagocytosis and/or phago-lysosome-directed pinocytosis. This phenomena, however, is blocked upon infection with *Mycobacterium tuberculosis* and the cells at this stage start serving as sanctuary for the lodging and growth of bacteria. Intracellular location of the bacteria protects them from the host defense mechanisms and restricts the penetration of antibiotics (2,3). It is, therefore, necessary to maximize the drug uptake by AMs for an efficient sterilization of microbial load. Once targeted, cells themselves could serve as a vehicle from where drug would be released via systematic biodegradation of the carrier system. However, inadequate specificity for macrophages and poor internalization potential of carriers constitute critical obstacles to the success of such delivery systems (4).

Macrophages possess mannose-specific membrane receptors which can recognize and facilitate the internalization of carriers bearing mannose residues (5). Unlike other glycoprotein receptors, mannose receptors mediate both, phagocytosis of saccharide-coated carriers as well as pinocytosis of soluble glycoconjugates (6). Therefore, much effort has been directed towards development of ligand-decorated carrier systems for cell-selective targeting to macrophages. Such carriers are efficiently phagocytosed by AMs and deliver a high payload of drug in comparison to the conventional dosage forms (7–9).

Isoniazid (INH), a first-line antitubercular drug, is characterized by its short half-life ranging from 1 to 4 h and tendency to form non-absorbed condensation products with the aldehyde and ketone groups of sugars (10). Besides, increased postprandial gastric pH results into further decrease in its bioavailability (11). Hence, an alternative route of INH delivery is highly desirable as it could avoid its intestinal metabolism, reduce the total dose delivered, and bring about improvement in bioavailability by modifying the pharmacokinetics and biodistribution profile.

Among various multiparticulate carrier systems, microparticles offer a higher drug payload especially for hydrophilic drugs and have a better ability to provide controlled release characteristics (12). In the present investigation, mannosylated gelatin microspheres (m-GMs) were developed to target alveolar macrophages and maintain the therapeutic concentration of INH for prolonged period of time. *Ex vivo* uptake of the microcarriers by AMs and their pharmacokinetics following pulmonary administration to rats were

[1] Department of Pharmaceutics, Institute of Technology, Banaras Hindu University, Varanasi, (U.P.), 221005, India.
[2] Department of Medicinal Chemistry, Institute of Medical Sciences, Banaras Hindu University, Varanasi, (U.P.), 221005, India.
[3] To whom correspondence should be addressed. (e-mail: bmishrabhu@rediffmail.com)

investigated. Gelatin was used as drug delivery matrix owing to its biodegradability, biocompatibility, non-immunogenicity, ease of modifying the functionality and tendency of enhancing phagocytic uptake by macrophage cells (13–15). It is expected that mannosylation of gelatin would enable the homing of carrier system to AMs whereas multiparticulate nature of the formulation would help in its spread within the lung environment and in sustaining the release rate of INH to prolonged period of time.

MATERIALS AND METHODS

Materials

INH was received as a gift sample from Macleod Pharmaceuticals, Mumbai. 4-(2-Hydroxyethyl)-1-piperazineethanesulfonic acid (HEPES) buffer and gelatin were purchased from Central Drug House, New Delhi. Trichloro acetic acid (TCA), ammonium acetate, RPMI 1640, and fluorescein sodium were purchased from Hi Media, Mumbai. Mannose was purchased from SD Fine Chemicals, Mumbai. Culture plates were purchased from Tarsons Products Ltd., Kolkata. Acetonitrile was purchased from Merck Ltd., Mumbai. Other solvents and chemicals were procured from manufacturers and used as received.

Animals

Male albino rats (Charles Foster strain; mean weight, 210 g) were procured from the Central Animal House, Banaras Hindu University. All procedures using animals were reviewed and approved by the Institutional Animal Ethical Committee of the Banaras Hindu University. Animals were allowed free access to tap water and standard pelleted diet. They were housed in plastic cages and maintained on a 12 h light/dark cycle at room temperature (21–25°C) and relative humidity of 45–55%.

Methods

Preparation of Mannosylated Gelatin Microspheres

Mannosylation of gelatin was performed by the method reported by Jain *et al.* (16). The resulting product was purified by dialyzing (thickness, 0.025 mm; molecular weight cutoff, 6,000–8,000 Da) against distilled water for 72 h. An excess of acetone was added drop wise into the dialysate to induce desolvation and precipitation of mannosylated gelatin (m-G). After lyophilization, it produced a light yellow powder.

m-GMs were prepared by emulsification solvent extraction method (15). Aqueous solution (5 ml; 5% *w/v*) of the lyophilized m-G, maintained at 60°C, was emulsified with soya oil (10 ml) preheated to the same temperature. INH was dissolved in aqueous phase. The emulsion was rapidly cooled to 5°C, which resulted into flocculation of the dispersed phase and production of microspheres. They were dehydrated by the addition of precooled acetone (5°C, 15 ml) under magnetic stirring for additional 30 min. Microspheres were finally filtered, washed with acetone, and vacuum dried. GMs were also prepared by the same method except that unmodified gelatin was used for their preparation.

Physicochemical Characterizations of Mannosylated Gelatin and Prepared Microspheres

Assessment of mannosylation was performed through Fourier transform infrared spectroscopy (FTIR) and nuclear magnetic resonance (NMR) spectroscopic studies. FTIR spectra of the samples were recorded over the range of 4,000–400 cm^{-1} using KBr disk method (Schimadzu, Model 8400, Japan). H^1-NMR spectra were recorded using Jeol AL300 FT-NMR spectrometer operating in the pulsed FT mode at a 300-MHz resonance frequency for protons. Samples were dissolved in D_2O and spectra acquisition was performed at constant temperature maintained throughout.

Volume-averaged diameter (V_d), size distribution, and zeta potential of the prepared microspheres were measured with a light scattering particle sizer (Beckman Coulter, Delsa™ Nano, USA). Other physical parameters, such as size, entrapment efficiency (percent EE), and drug loading (DL) were also evaluated.

In Vitro Release of INH from the Prepared Formulation

In vitro drug release studies were independently conducted in two media; MacIlvein buffer solution (MBS) at pH 4 and phosphate-buffered solution (PB) at pH 7.4. The former was used to simulate the pH conditions prevailing within phagolysomes while latter mimicked the case when the formulation was in cytosol (17). Formulation equivalent to 5 mg free drug was placed in the egg shell membrane which was prepared from the fresh chicken egg as per the method described elsewhere (18). The membrane was hermetically sealed and immersed into a 25-ml beaker containing 10 ml release media maintained at 37±0.5°C and stirred at 50 rpm. Samples of 1 ml were collected at prespecified time intervals and media was immediately restored with the same volume of prewarmed fresh buffer. Drug content was analyzed spectrophotometrically at 262 nm (Shimandzu 7800, Tokyo, Japan). The study was conducted in triplicate.

High-Performance Liquid Chromatographic Analysis of INH

The concentration of INH in rat plasma was determined by the method described elsewhere (19), with slight modification. Plasma (50 μl) containing isoniazid was extracted with 100 μl of 10% TCA by vortexing for 30 s. It was then centrifuged (14,000 rpm/10 min). The supernatant was withdrawn and half diluted with ammonium acetate buffer (0.5 M, pH 8.20) so as to neutralize the excess TCA. This solution mixture (25 μl) was injected to high-performance liquid chromatography (HPLC) system (Cecil CE4201, Cambridge, UK), equipped with C-18 column (Phonomenex, 250× 4.60 mm, particle size 5 μm) and UV visible detector.

Isocratic mobile phase was composed of acetonitrile and ammonium acetate (10 mM; pH 4.5) in the ratio of 10:90 (vol/vol). Elution was performed at 30°C with a flow rate of 1 ml/min (pressure, 25 bar) and run time of 7 min. Under these conditions, retention time for INH at operating wavelength 262 nm was observed to be 4.1 min. The column was re-equilibrated to starting conditions for 4 min. Drug was quantified by comparison of its peak area to the peak area obtained from an aqueous INH standard. Values were

corrected for the appropriate dilutions and calculated as microgram per millilitre. Precision and accuracy of the method were evaluated by adding quality control samples to the blank plasma. Standard curve for INH was found to be linear in the range of 5–200 ng/ml (r^2=0.99).

Ex Vivo Drug Accumulation Studies in Cultured Alveolar Macrophages

Animals were deeply anesthetized with pentobarbitone (30 mg/Kg), injected intraperitoneally, and AMs were harvested by broncheo-alveolar lavage. A polyethylene tube was inserted into the trachea and tied along with it. Through the use of a 1-mL syringe with a needle inserted in the tube, the lungs were lavaged 10 times with 2 ml aliquots of Ca^{2+} and Mg^{2+}-free Hank's balanced salt solution (5). The lavaged cell suspension was centrifuged at 4°C and the pellet was resuspended in HEPES buffer. Cell viability was checked by tryptan blue exclusion test (20). Cells were treated with 100 µl of 0.4% dye solution and counted with Neubauer hemocytometer. Cells appearing blue were considered dead whereas viable cells excluded the dye. Cells with seeding density of 1×10^6 cells/mL were plated in 12-well culture plates in RPMI 1640 supplemented with 10% fetal calf serum and 1% antibiotics. After overnight incubation at 37°C and 5% CO_2, the cells were treated with free INH, GMs, and m-GMs at the same dose level (21). In a parallel experiment, 0.05 M mannose, a corresponding sugar inhibitor, was added to observe its effect on the cell internalization behavior of m-GMs.

The study was terminated at the end of 24 h. Cells were removed from the wells and subjected to two cycles of washing/centrifugation (5,000 rpm/3 min) with ice-cold phosphate-buffered saline (PBS) containing 20 mM ethylenediaminetetraacetic acid (1). Supernatants were pooled together to quantify the surface bound drug. For the estimation of intracellular drug concentration, cell pellet, stored at −80°C, was homogenized by resuspension in distilled deionized water (100 µl) and sonicated on ice (three cycles/60 s; 21). Intracellular and extracellular drug concentrations were estimated by HPLC method.

Confocal laser scanning microscopy was used to visualize the interaction of microspheres with macrophage cells. Microspheres (2,000 µg/well), labeled with fluorescein sodium, were added to the culture plates containing the previously harvested AMs. They were incubated for 2 h at 37°C and 5% CO_2. Cells were finally fixed with an aqueous solution of 8% *v/v* formaldehyde and examined under confocal microscope (510 META, Zeiss, Germany).

Stability of the Formulation in Broncheo-Alveolar Lavage Fluid

Broncheo-alveolar lavage fluid (BALF) was collected from the animals with ice-cold phosphate-buffered saline (pH 7.4) using the protocol described above. AMs were removed by immediate cold centrifugation (10,000 rpm/5 min) of BALF and supernatant was collected. Two milligram formulation (m-GMs) was dispersed with 1 ml supernatant through vortexing for 30 s. The sample was stored for 48 h at 4°C and was examined under scanning electron microscope (SEM).

Pharmacokinetic Studies

Animals were divided into three groups, each group containing six animals (n=6). Animals of group II and III received GMs and m-GMs, respectively, through intratracheal instillation (5). Animals were deeply anesthetized and a small hole was made between the fifth and sixth tracheal rings using a 20-gauge needle. Following this, trachea was cannulated with a polyethylene tube. Formulation was dispersed in 500 µl PBS (pH 7.4) through vortex mixing for 30 s. It was then instilled slowly over a period of 1 min using a 1-mL syringe attached to the polyethylene tube (22). Group I animals were administered with drug solution and they served as control. Volume of vehicle and dose level (5 mg) were kept constant in each case. At prespecified time intervals (t=0, 0.5, 1, 2, 4, 8, 16, and 24 h), serial blood samples of approximately 200 µl were withdrawn from the retro-orbital plexus under mild ether anesthesia. Blood samples were cold centrifuged (10,000 rpm/10 min) and the separated plasma was analyzed by the above stated HPLC method.

Estimation of pharmacokinetic parameters was performed using Kinetica 5.0 (Trial Version). Maximum plasma concentration (C_{max}), time to achieve C_{max} (T_{max}), and mean residence time (MRT) were calculated. Area under plasma concentration–time curve $[AUC]_{0-48}$ was determined by trapezoidal method till last measurement point and was extrapolated to infinity $[AUC]_{0-\infty}$.

Statistical Analysis

Results were subjected to one-way analysis of variance (ANOVA). P values less than 0.05 were considered significant.

RESULTS AND DISCUSSION

Physicochemical Characterizations of Mannosylated Gelatin and Prepared Microspheres

FTIR spectra of gelatin exhibited medium absorption near 3,400 cm^{-1}, which is indicative of presence of primary amino group. Also, it showed typical C–H stretching frequencies at about 3,000 cm^{-1} (Fig. 1a). On the other hand, mannosylated gelatin showed medium C=O absorptions in the range of 1,680–1,630 cm^{-1}, which is indicative of presence of primary and secondary amides (16). Emergence of amide groups provides the evidence that coupling between –CHO groups of mannose and $–NH_2$ groups of gelatin occurred via Schiff base formation. A broad O–H stretching vibration was observed in the range from 3,400 to 3,300 cm^{-1}. It could be attributed to the presence of alcoholic groups of mannose in its open chain form (Fig. 1b).

Figure 2 shows high resolution H^1-NMR spectra of gelatin before and after mannosylation. In case of gelatin, most of the proton signals are well resolved within the region of chemical shifts ranging from 0.77 to 3.78 ppm. They could be assigned to the methyl resonances of specific amino acids

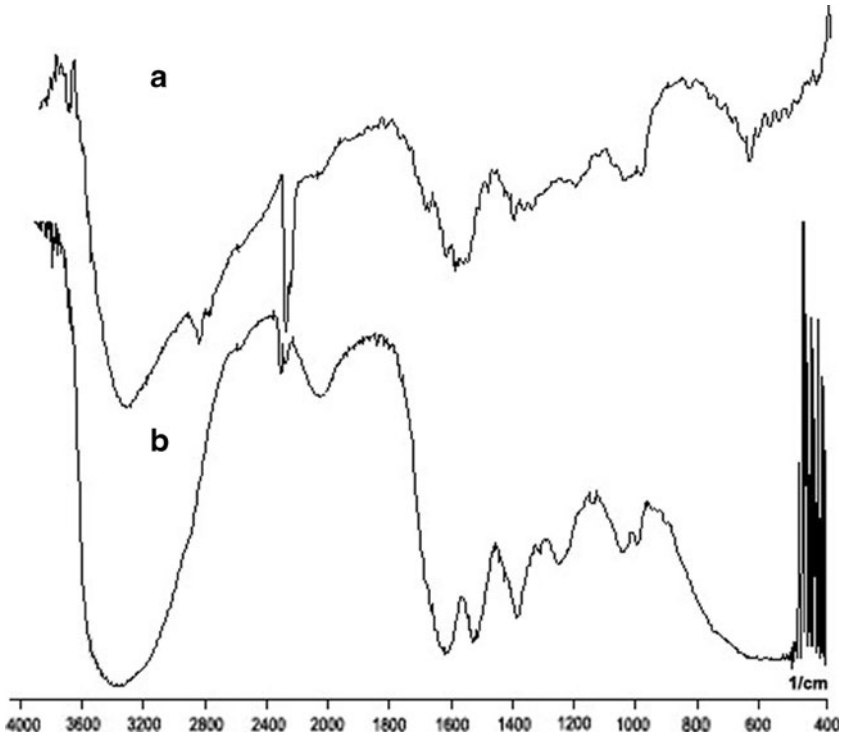

Fig. 1. FT-IR spectra of: *a*) unmodified gelatin, *b*) lyophilized mannosylated gelatin (Data were collected over 50 scans at 4° resolution)

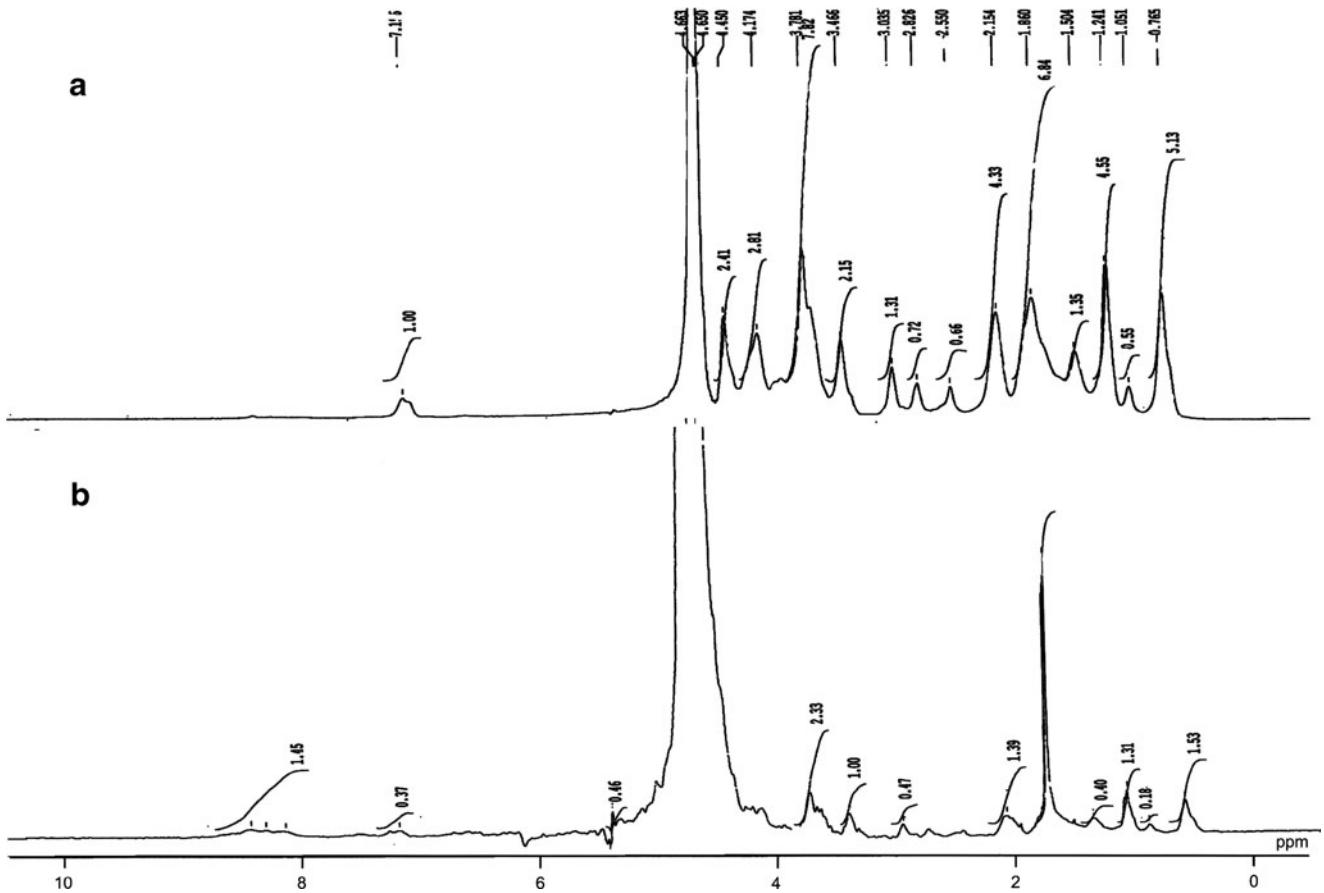

Fig. 2. H^1-NMR spectra of: *a*) unmodified gelatin, *b*) lyophilized mannosylated gelatin

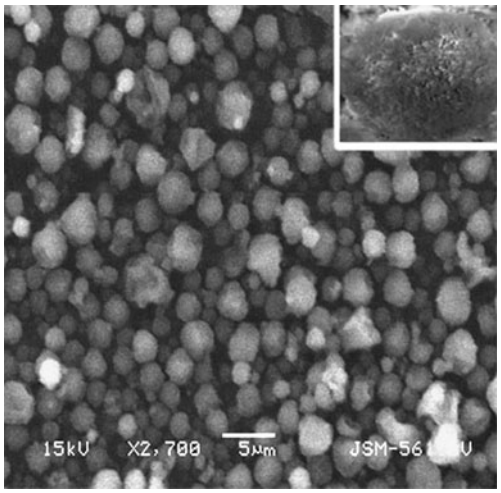

Fig. 3. Mannosylated gelatin microspheres as visualized by scanning electron microscopy (1 mg microspheres were mounted on an aluminum support, sputter-coated, and analyzed at an operation voltages of 15 and 5 kV (Philips XL-20, Holland); figure provided in the *inset* represents a single microsphere showing its porous structure)

and paired protons of $–CH_2–$ and $–NH_2$ groups present in the molecular structure of gelatin (23). The central intense line could be attributed to the superposition of H^1 signals derived from –OH and $–CH_3$ groups. A relatively weaker signal detected at 7.16 ppm could be attributed to the presence of aromatic ring (Fig. 2a). m-GMs showed specific line broadening and decrease in the integral intensity of spectral lines in the region of aminoacids, i.e., 0.77–3.78 ppm. It was thus concluded that aminoacids played a vital role in the mannosylation of gelatin and it would have occurred via interaction between aldehyde group of mannose and amino group of gelatin. A broader line detected at 4.65 ppm could be due to conversion of –CHO to –OH groups during ring opening of mannose (Fig. 2b).

The morphology of resulting microspheres was observed by SEM (Fig. 3). They were of spherical shape with slightly irregular surface profile. Certain invaginations could also be observed on their surface. SEM image provided in the inset shows the porous character of the microspheres. V_d of microspheres ranged from 0.1 to 6 μm and they were well dispersed as individual particles. Mean V_d of GMs and m-GMs was found to be 1.82 μm (±1.94) and 3.89 μm (±3.23), respectively, which could be deemed suitable for their delivery to the AMs (24). Zeta potential, EE, and DL of m-GMs were 12.37±3.26 mV, 55.92±2.40%, and 18.38±1.08%, respectively. Corresponding values for GMs were found to be 17.37±5.38 mV, 58.09±3.71%, and 14.29±5.34%, respectively. Thus, no significant difference was found between GMs and m-GMs with respect to their size, zeta potential, EE, and DL ($p>0.05$).

In Vitro Drug Release

In vitro release profiles of INH have been shown in Fig. 4. As can be seen from the release profiles in PB, sustained release pattern was evident from the formulations as compared to free drug. The effect could probably be due to time-dependent swelling of the microsphere matrix. Swelling resulted into reduction of external surface and a simultaneous increment in the diffusional path length of drug molecules. Under *in vitro* testing conditions, more than 90% drug release

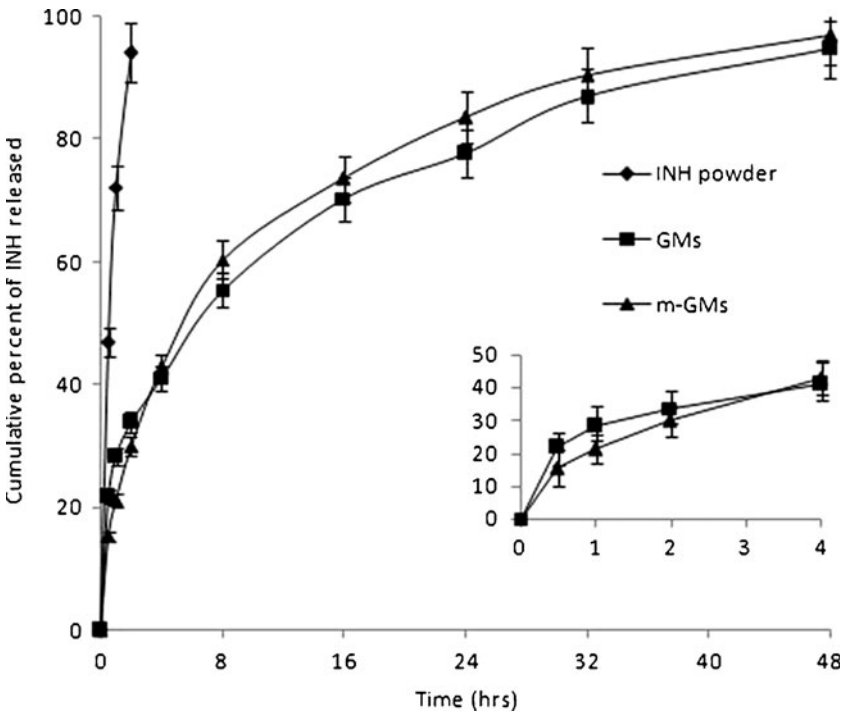

Fig. 4. *In vitro* release of INH from the prepared microspheres (inset provides the *in vitro* dissolution profiles of GMs and m-GMs for the initial 4 h; *bars* represent ±standard deviation; $n=3$)

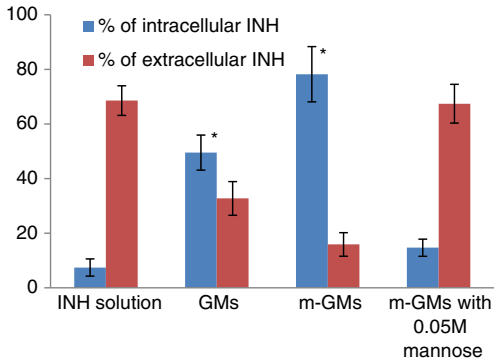

Fig. 5. *Ex vivo* drug uptake by the cultured alveolar macrophages over a period of 24 h (*bars* represent ±standard deviation; $n=3$). *Asterisk* represents significant difference in the percentage of internalized drug as compared to INH solution

occurred from both, GMs and m-GMs and no significant difference was observed in their release rates ($p>0.05$). Initially, release rate was slightly higher from GMs; 34% INH was released during first 2 h as against to 30% released from m-GMs. However, the difference was not found significant ($p>0.05$). The remaining amount of drug was released at an approximately similar rate up to 48 h from both the formulations. Literature reports suggest that macrophages take 2 h to achieve their maximum engulfment capacity (25). Therefore, it can be deduced that the majority of drug would be released inside the cell following endocytosis of the carrier system. Drug release studies conducted in MBS did not differ significantly to the results of PB (data not shown; $p>0.05$). It can thus be presumed that release of INH from the prepared formulations would not be influenced by pH of the release media.

Ex Vivo Drug Uptake Studies

Internalization efficiency of the ligand directed carriers can be correlated to their therapeutic efficacy. Therefore, uptake of the developed formulation was studied in cultured alveolar macrophages and the results are depicted in Fig. 5. Formulations exhibited significantly higher uptake of INH as compared to drug solution ($p<0.05$), which is consistent to the literature reports (21,26). This effect is very obvious with the view that drug solution will have a tendency of undergoing distribution rather than being internalized specifically by the cells. Microspheres, being opsonic materials, would be natural substrates for the uptake by AMs. Eventually, m-GMs exhibited significantly higher intracellular concentration of INH than GMs ($p<0.05$; one-way ANOVA). Recognition pattern offered by mannosylated carriers would have led to their specific binding and stable adsorption to mannose-specific membrane receptors of AMs, which subsequently might have resulted into their higher uptake (27). Addition of mannose to the culture media resulted into significant reduction in drug uptake through mannosylated carriers ($p<0.05$). It provided us the proof-of-principle that uptake of mannosylated carriers occurred via mannose receptor mediated endocytosis.

As can be observed from Fig. 5, intracellular and extracellular INH bars added to approximately 80% for INH solution whereas bars for other systems added to about 95%. This was suggestive of loss of about 20% drug in case of INH solution and some minimal loss in other cases. We attributed this loss to the metabolism of INH within macrophage cells. It is worth mentioning that free drug would be more prone to metabolism as compared to the drug entrapped within the delivery system. Our observations corroborated to the findings of Muttil *et al.* (28). Another study which, though is not specific to INH, also provided the evidence of metabolic activity of cultured macrophage cells (29). On the other hand, Jayaram *et al.* reported that INH remains stable in macrophage cultures (19). Therefore, data of INH metabolism in uninfected macrophage culture are contradictory and further studies are warranted to explore this aspect.

Confocal microscopy showed a more accurate comparison between the unmodified and ligand-directed microparticles since direct interaction of the formulation with

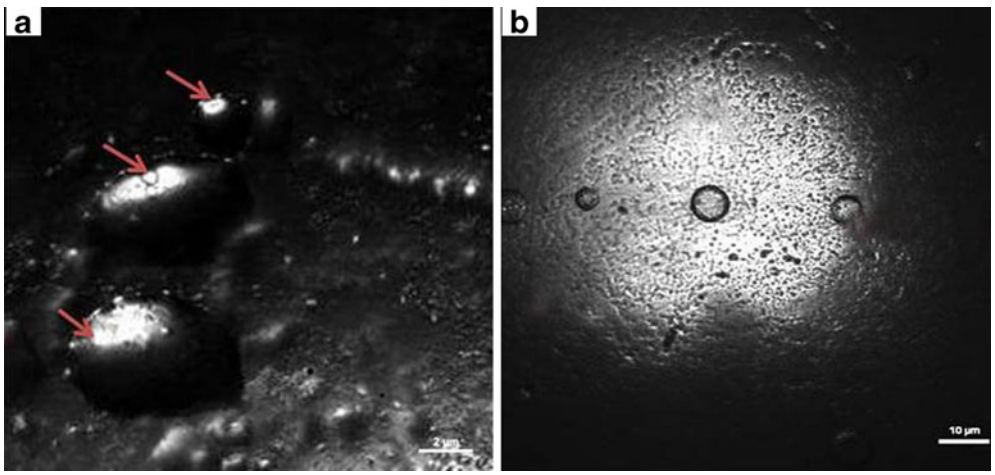

Fig. 6. Bright field confocal lazer scanning microscopic image showing endocytosis of m-GMs in AMs, cultured for 2 h in RPMI 1640. Phago-lysosomes containing microspheres have been marked with *arrows*. Scanning was performed using 20× Plan Aprochromat objective, having a numerical aperture of 0.8. Images were acquired at an excitation wavelength of 488 nm and band pass of 505–550 nm. Twenty percent of the maximum power was used

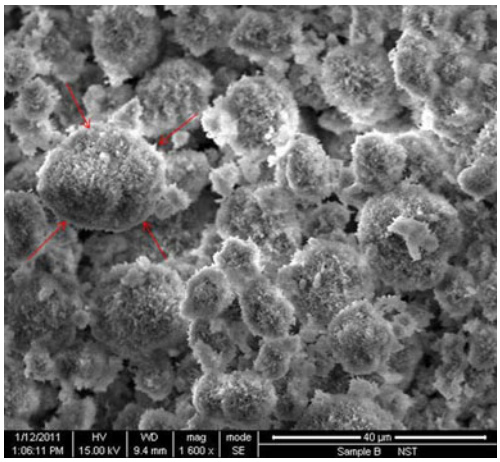

Fig. 7. Scanning electron microscopic image of microspheres (m-GMs) incubated for 48 h with the harvested broncheo-alveolar lavage fluid. *Arrows* indicate the possible ring of lung surfactant

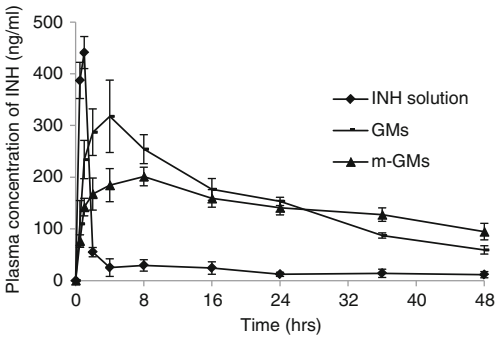

Fig. 8. Plasma concentration *vs.* time profile of microspheres administered to rats (*bars* represent ±standard deviation; $n=3$)

macrophage cells was taken into account. It supplemented the results obtained with the drug uptake studies, showing a higher number of m-GMs associated with macrophage cells as compared to GMs. m-GMs exhibited strong fluorescence due to the internalization of microparticles inside the cells. Some adsorbed particles can also be visualized around the macrophage cells (Fig. 6a). Control experiments with GMs, however, did not show such pattern of fluorescence due to their lower interaction potential with the cell membrane receptors (Fig. 6b). These fluorescence patterns can be qualitatively correlated with the interaction of mannosylated carrier systems with the macrophage surface receptors and their facilitated internalization to a higher extent (30).

Stability of the Prepared Formulation in BALF

Figure 7 shows the SEM image of mannosylated formulation in BALF. In contact with BALF, microspheres slightly grew in size and their surface became much smoother. Particles maintained their integrity except that they showed slight clustering. However, there occurred no entanglements among the particles. It could be attributed to the presence of pulmonary surfactant in the BALF, which would have created a protective layer at interface of particles and prevented their aggregation (17). A marked ring of stabilizing surfactants surrounding the particles can be viewed in the micrograph. Smaller remnants, scattered here and there, probably represent the artifacts of macrophage cells. It was inferred from these results that the formulation was sufficiently stable in the microenvironment of AMs.

Pharmacokinetic Studies

Pharmacokinetic data presented in Table I were indicative of sustained maintenance of INH concentration in the plasma. Though GMs provided a higher value of AUC_{0-48h} as compared to m-GMs, yet the difference was not significant ($p>0.05$). m-GMs resulted into significant improvement in the value of MRT and $AUC_{0-\infty}$ ($p<0.05$). Thus, performing mannosylation of the carrier systems not only improved their targeting potential to AMs, but their persistence within the biological system was also enhanced. Free INH solution delivered directly to the lungs resulted into faster achievement of peak drug level (60 min) in the plasma (Fig. 8). Its concentration, however, declined quickly due to rapid clearance from blood. During absorption phase, plasma concentration of INH following administration of both, GMs and m-GMs, remained significantly lower than that of free drug solution at each time point ($p<0.05$). It probably occurred owing to the specific and/or non-specific uptake of carriers by AMs. As a result, there was a restricted and sustained distribution of INH into blood and no sharp peaks were realized in their pharmacokinetic profile.

Upon administration of GMs, maximum concentration of INH (C_{max}) was observed at 4 h. Plasma level of INH from m-GMs remained lower than that of GMs throughout the study period. Administration of m-GMs resulted into up regulation of mannose receptors which would have

Table I. Comparison of Pharmacokinetic Parameters of INH, Following Pulmonary Administration of Microsphere Formulations and Drug Solution to Rats

Dosage form	C_{max} (ng/ml)	T_{max} (h)	AUC_{0-48h} (ng h/ml)	$AUC_{0-\infty}$ (ng h/ml)	MRT (h)
INH solution	441.09 (±28.21)	1.0	1,412.965 (±352.31)	1,904.196 (±257.42)	–
GMs	317.75 (±40.19)	4.0	7,485.868 (±537.06)	9,037.948 (±785.64)	27.352 (±2.71)
m-GMs	201.34 (±13.58)	8.0	6,939.778 (±413.21)	12,590.766 (±659.87)	59.55 (±6.24)

The data represent mean value of three experiments. Values provided in the bracket represent standard deviation of mean values ($n=3$). *MRT* means residence time

triggered their preferential uptake by AMs (26). Consequent to this, much lower plasma concentration was provided by them. These results are consistent to the previous findings on mannosylated gelatin nanoparticles of didanosine (16).

CONCLUSION

The present study illustrated the potential of mannosylated gelatin microparticles to target the alveolar macrophages. FTIR and H^1-NMR spectral analysis convinced us that mannosylation occurred through coupling between aldehyde group of mannose and amino group of gelatin. The delivery system was prepared by a simple formulation approach, utilizing a cost-efficient, biodegradable, and Food and Drug Administration-approved polymer. Prepared microparticles presented suitability for physicochemical characteristics, such as size, shape, zeta potential, and drug loading. Pharmacokinetic studies showed that the formulation could achieve therapeutic concentration of INH and maintain it for prolonged period of time with a fairly reduced clinical dose. It was concluded from this study that ligand-decorated carriers could be a potential strategy to improve the therapeutic properties of antitubercular drugs.

ACKNOWLEDGMENTS

First author acknowledges the financial assistance of Council of Scientific and Industrial Research, New Delhi, in carrying out this research work. The support of Prof. ON Srivastava (Department of Physics) and Prof. SC Lakhotia (Department of Zoology) of Banaras Hindu University is thankfully acknowledged for providing the facility of SEM and confocal laser scanning microscopy studies, respectively.

Declaration of interest The authors report no conflicts of interest. The authors alone are responsible for the content and writing of the paper.

REFERENCES

1. Wijagkanalan W, Kawakami S, Takenaga M, Igarashi R, Yamashita F, Hashida M. Efficient targeting to alveolar macrophages by intratracheal administration of mannosylated liposomes in rats. J Control Rel. 2008;125:121–30.
2. Roseeuw E, Coessens V, Balazuc AM, Lagranderie M, Chavarot P, Pessina A, *et al*. Synthesis, degradation, and antimicrobial properties of targeted macromolecular prodrugs of norfloxacin. Antimicrob Agents Chemother. 2003;47:3435–41.
3. Briones E, Colino CI, Lanao JM. Delivery systems to increase the selectivity of antibiotics in phagocytic cells. J Control Rel. 2008;125:210–27.
4. Yeeprae W, Kawakami S, Yamashita F, Hashida M. Effect of mannose density on mannose receptor-mediated cellular uptake of mannosylated o/w emulsions by macrophages. J Control Rel. 2006;114:193–201.
5. Liang WW, Shi X, Deshpande D, Malanga CJ, Rojanasakul Y. Oligonucleotide targeting to alveolar macrophages by mannose receptor-mediated endocytosis. Biochim Biophys Acta. 1996;1279:227–34.
6. Dong L, Xia S, Luo Y, Diao H, Zhang J, Chen J, *et al*. Targeting delivery oligonucleotide into macrophages by cationic polysaccharide from *Bletilla striata* successfully inhibited the expression of TNF-α. J Control Rel. 2009;134:214–20.
7. Dutta M, Bandyopadhyay R, Basu MK. Neoglycosylated liposomes as efficient ligand for the evaluation of specific sugar receptors on macrophages in health and in experimental leishmaniasis. Parasitology. 1994;109:139–47.
8. Vyas SP, Katare YK, Mishra V, Sihorkar V. Ligand directed macrophage targeting of amphotericin B loaded liposomes. Int J Pharm. 2000;210:1–14.
9. Sou K, Goins B, Takeoka S, Tsuchida E, Phillips WT. Selective uptake of surface-modified phospholipids vesicles by bone marrow macrophages *in vivo*. Biomaterials. 2007;28:2655–66.
10. Holdiness MR. Clinical pharmacokinetics of the antituberculous drugs. Clin Pharmacokinet. 1984;9:511–44.
11. Weber WW, Hein DW. Clinical pharmacokinetics of isoniazid. Clin Pharmacokinet. 1979;4:401–22.
12. Brandhonneur N, Chevanne F, Vie V, Frisch B, Primault R, Potier MFL, *et al*. Specific and non-specific phagocytosis of ligand-grafted PLGA microspheres by macrophages. Eur J Pharm Sci. 2009;36:474–85.
13. Wang J, Tabata Y, Morimoto K. Aminated gelatin microspheres as a nasal delivery system for peptide drugs: evaluation of *in vitro* release and *in vivo* insulin absorption in rats. J Contol Rel. 2006;113:31–7.
14. Morimoto K, Chono S, Kosai T, Seki T, Tabata Y. Design of cationic microspheres based on aminated gelatin for controlled release of peptide and protein drugs. Drug Deliv. 2008;15:113–7.
15. Adhirajan N, Shanmugasundaram N, Shanmuganathan S, Babu M. Functionally modified gelatin microspheres impregnated collagen scaffold as novel wound dressing to attenuate the proteases and bacterial growth. Eur J Pharm Sci. 2009;36:235–45.
16. Jain SK, Gupta Y, Jain A, Saxena AR, Khare P, Jain A. Mannosylated gelatin nanoparticles bearing an anti-HIV drug didanosine for site-specific delivery. Nanomedicine: NBM. 2008;4:41–8.
17. Tomoda K, Makino K. Effects of lung surfactants on rifampicin release rate from monodisperse rifampicin-loaded PLGA microspheres. Coll Surf B: Biointerf. 2007;55:115–24.
18. Philip AK, Singh N, Pathak K. Egg shell membrane as a substrate for optimizing *in vitro* transbuccal delivery of glipizide. Pharm Dev Tech. 2009;14:540–7.
19. Jayaram R, Shandil RK, Gaonkar S, Kaur P, Suresh BL, Mahesh BN, *et al*. Isoniazid pharmacokinetics-pharmacodynamics in an aerosol infection model of tuberculosis. Antimicrob Agents Chemother. 2004;48:2951–7.
20. Torres-Lugo M, Garcia M, Record R, Peppas NA. Physicochemical behavior and cytotoxic effects of p(methacrylic acid-g-ethylene glycol) nanospheres for oral delivery of proteins. J Control Rel. 2002;80:197–205.
21. Zhou H, Zhang Y, Biggs DL, Manning MC, Randolph TW, Christians U, *et al*. Microparticle-based lung delivery of INH decreases INH metabolism and targets alveolar macrophages. J Control Rel. 2005;107:288–99.
22. Surti N, Misra AN. Wheat germ agglutinin-conjugated nanoparticles for sustained cellular and lung delivery of budesonide. Drug Deliv. 2008;15:81–6.
23. Zandi M, Mirzadeh H, Mayer C. Early stages of gelation in gelatin solution detected by dynamic oscillating rheology and nuclear magnetic spectroscopy. Eur Poly J. 2007;43:1480–6.
24. Hirota K, Hasegawa T, Hinata H, Ito F, Inagawa H, Kochi C, *et al*. Optimum conditions for efficient phagocytosis of rifampicin-loaded PLGA microspheres by alveolar macrophages. J Control Rel. 2007;119:69–76.
25. Cannon GJ, Swanson JA. The macrophage capacity for phagocytosis. J Cell Sci. 1992;101:907–13.
26. Chono S, Tanino T, Seki T, Morimoto K. Efficient drug targeting to rat alveolar macrophages by pulmonary administration of ciprofloxacin incorporated into mannosylated liposomes for treatment of respiratory intracellular parasitic infections. J Control Rel. 2008;127:50–8.
27. Ahsan F, Rivas IP, Khan MA, Suarez AIT. Targeting to macrophages: role of physicochemical properties of particulate

carriers—liposomes and microspheres—on the phagocytosis by macrophages. J Control Rel. 2002;79:29–40.
28. Muttil P, Kaur J, Kumar K, Yadav AB, Sharma R, Misra A. Inhalable microparticles containing large payload of anti-tuberculosis drugs. Eur J Pharm Sci. 2007;32:140–50.
29. Cheu J, Talaska G, Miller M, Rice C, Warshawsky D. Benzo[*a*] pyrene coated ferric oxide and aluminum oxide particles: uptake, metabolism and DNA binding in hamster pulmonary alveolar macrophages and tracheal epithelial cells *in vitro*. Carcinogenesis. 1996;18:167–75.
30. Jiang HL, Kang ML, Quan JS, Kang SG, Akaike T, Yoo HS, *et al*. The potential of mannosylated chitosan microspheres to target macrophage mannose receptors in an adjuvant-delivery system for intranasal immunization. Biomaterials. 2008;29:1931–9.